ANEXA 1.A

Call: 2024 **Project acronym: CEHDEP**

FAIR Research Programme / Experiment: *CBM*

Annual Summary Document[1]

Year: 2025

Months: 12

Project Title:

CBM experiment on the horizon - detectors, electronics, data acquisition and physics/CEHDEP

Project Work Plan (according to the contract)

Stage: II. *Contribution of DFH in 2025, through research and development activities, on the way towards the materialization of the CBM experiment at FAIR.*

Activities:

Updated design of the inner zone of CBM ToF subsystem based on the architecture of the direct flow MSMGRPC.

Correlated analysis of CBM formatted TRD-2D data measured in the mCBM setup with STS and ToF detectors for a unbiased characterization of the position and energy resolution.

Versatile motherboard for testing large amount of encapsulated FASP CHIPs from production engineering. Firmware optimization of the new front-end board for the TRD-2D in correlation with its usage on the detector in CBM.

Extensive tests of the performance of the direct flow MSMGRPC equipped with the readout electronic chain designed and built for the inner zone of the CBM-TOF wall.

1Please fill in all the required items and do not alter the template

- Specify scientific focus of the group and role in the collaboration
  Contribution of DFH in 2025, through research and development activities, on the way towards the materialization of the CBM experiment at FAIR.
- Summary of accomplishments during the reporting period
  - Updated design drawings of the modular configuration of the CBM-TOF inner wall resulted from the implementation of the prototypes based on direct flow.
  - Software development for TRD-2D performance analysis, integrated in the CBMRoot packages: FEE calibration, local reconstruction, temporal and spatial alignment, tracking and finally position and energy performance estimation.
  - Successfuly test of the complete detection chain prepared for TRD2D readout, including the integration of the Front-End Electronics (FEE) based on the FASP ASIC in the common CBM-ready data taking,
  - Performance of the direct flow MSMGRPC based on discrete spacers, tested in the mCBM setup: efficiency 95% and performant time resolution (~50 ps).

2. Scientific accomplishments

- Results obtained during the reporting period

2.1 CBM - TOF

2.1.1 Updated design of the modular configuration of the CBM-TOF inner wall resulted from the implementation of direct flow MSMGRPCs

The CBM – TOF inner wall covers ~14 m^2 area bewteen 2.5^0 and 11^0 polar angles. The anticipated counting rate for this part of the TOF wall is ranging from challenging value of about 50 kHz/cm^2 in the region close to the beam pipe to about 5 kHz/cm^2 at the largest polar angle mentioned above. In the current design of the CBM-TOF wall, the inner zone area covers 4.5 m in x direction and 3 m in y direction, merging with the outer wall area. In the z direction its thickness is 0.6 m.

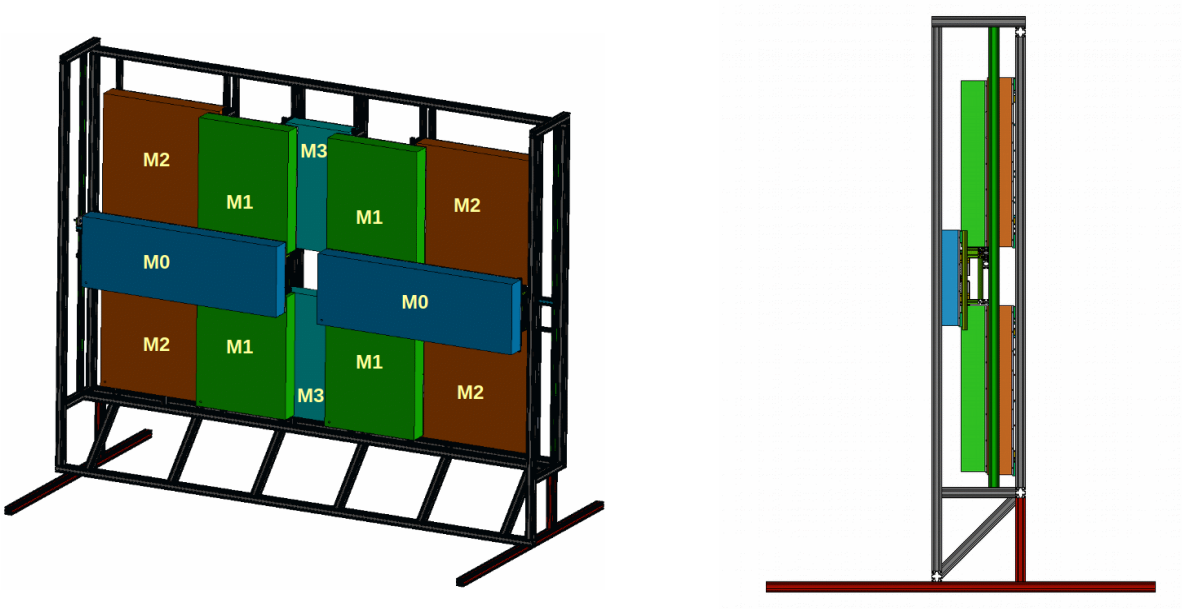

Fig.1 Modules of the CBM-TOF inner wall area (left – front view, right – side view).

The CBM-TOF inner zone design (see Fig.1) is the result of the optimization in terms of wall thickness along z direction with a minimum overlap between the chambers as well as between the modules, such to have a continuous coverage of the active area and not at least, correlated with the optimization of the costs in terms of number of chambers and electronic readout channels. All these constrains led to a modular concept defined by 12 modules of 4 types (M0, M1, M2, M3), staggered in z direction in order to assure the continuity of the active area through the overlap of the chambers between modules as well as inside each module.

A module is an independent box housing a certain numbers of direct flow MGMSRPCs, precisely positioned by mechnical supports. Each module contains up to three types of chambers. The chamber's type is defined only by its strip length (MRPC1a – 56 mm, MRPC1b – 96 mm and MRPC1c – 196 mm), chosen such to cover the granularity requirement at different polar angles, while the strip pitch and the inner geometry of the chambers are the same. Based on the criterias mentioned above, (minimization of the overlap of the active zone between the chambers as well as between the modules, together with a reduced material budget and number of electronics channels), the spatial configuration of the chambers inside a module was updated according with the latest design of the direct flow prototypes. In this latest architecture, in order to minimize the aging effects, the outermost spacers were positioned outside of the action of the electric field. For this reason the active area of each chamber was reduced by 6% for MRPC1a, 4% for MRPC1b and 2% for MRPC1c, shortening the length of the high voltage and readout strips with 4 mm in comparison with the old design (for more details, see reference 2).
Taking into consideration the new active area of each of the three types of MSMGRPCs the position of each chamber inside a module was adjusted and geometrical defined assuring the proper overlaps. Inside a module the chambers are staggered on four layers in z directions based on the mentioned criteria, as can be seen in Fig.2, Fig.3 and Fig.4. for the four modules types. The complex chamber puzzle seen in the mentioned figures is the result of the limitation in the maximum available size of the Chinese low resistivity glass to 300 mm length. The modules are staggered too, in both x and y directions, providing the overlaps of the active areas between the chambers of different modules.

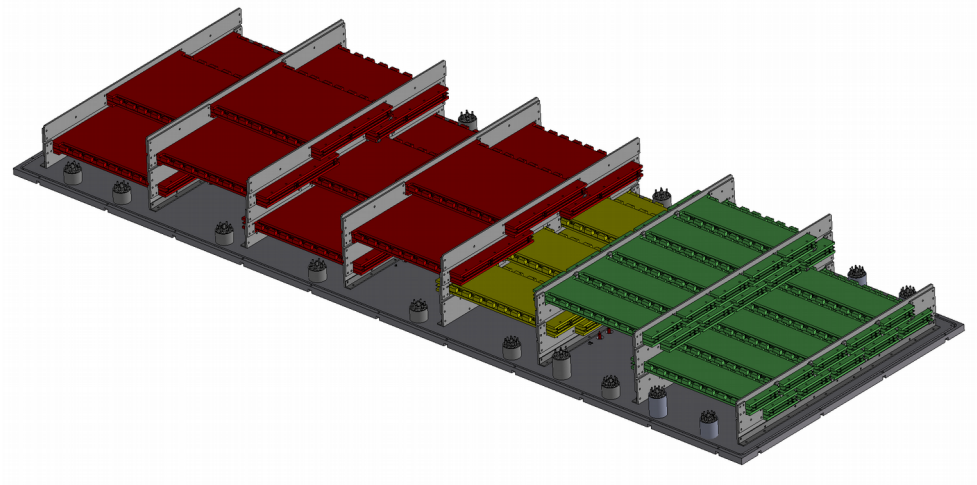

Fig.2 Module M0 design (green – MRPC1a, olive – MRPC1b, dark red MRPC1c).

In the new design, the modules have shrunk, modifying their sizes; i.e. module M0 changes its sizes from 2105 mm x 738 mm x 196 mm to 2064 mm x 685 mm x 163 mm.
The overlap of the chambers in the module M0 in x direction is of 26.5 mm for MRPC1a chambers, of 18.8 mm for MRPC1b/MRPC1a chambers and 35.5 mm between MRPC1b/MRPC1a and of 8 mm for MRPC1c. On the y direction, the overlap is of 5 mm for MRPC1a, of 7.36 mm for MRPC1b and of 19 mm for MRPC1c (where x and y are considered according with the CBM coordinate system). M0 module has the most complex configuration because it accommodates all three type of chambers.
The M1 module type, shown in Fig.3, accommodates 2 types of chambers, i.e MRPC1b and MRPC1c, while M2 modules (Fig.4) have implemented only MRPC1c chambers.

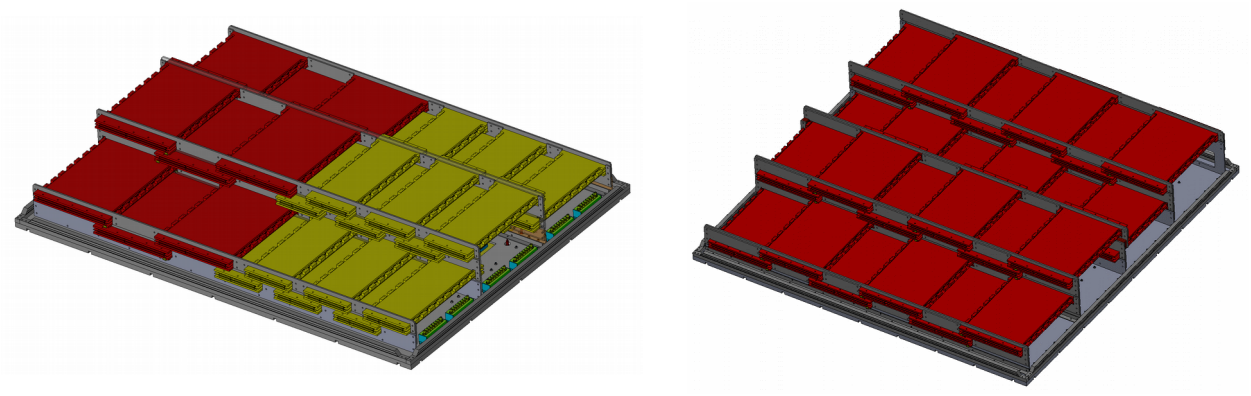

Fig.3 Module M1 -left and M2 -right designs (olive – MRPC1b, dark red MRPC1c).

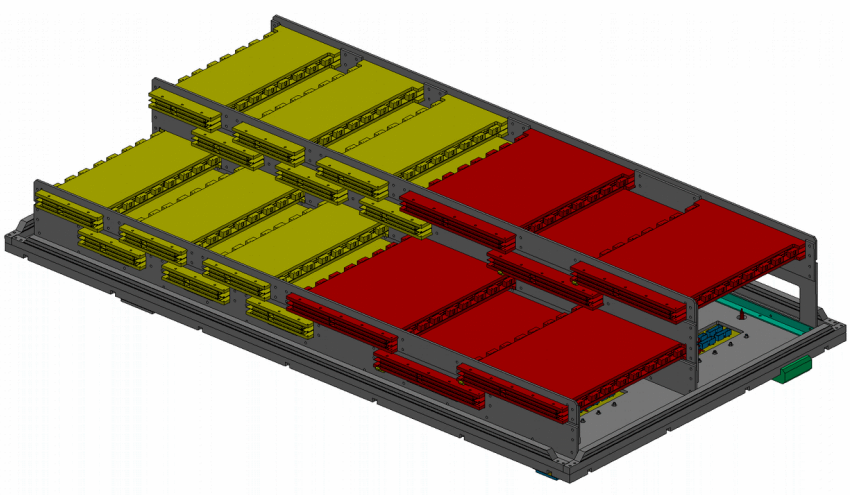

Fig.4 Module M3 design (olive – MRPC1b, dark red MRPC1c).

In addition, for the design of each module a special attention was paid to assure a proper gas distribution to each chamber, to feed them with high voltage of both polarities, as well as to route the signal cables from each MSMGRPC to the connectors positioned on the backpanel. Due to the high density of the readout channels for the chambers positioned at small polar angles, this issue is challenging. A cabling manual is in progress to have a

record of the proposed solution, it being applicable also to second M0 module. Based on the experience gained with the implementation of the services for the first M0 module, which will be documented in corresponding manuals, similar ones will be drafted also for the other modules.
A mechanical frame is designed and optimized in terms of material budget such to provide a precise and safe positioning of the modules.

2.1.2
Performance of the direct flow MSMGRPCs equipped with the readout electronic chain designed and build for the inner zone of the CBM-TOF wall.
A long term operation of a MSMGRPC in high counting rate leads to aging effects [1]. One of these effects is the increase of the noise rate, highlighted especially around the spacers (fishing line) [1], which could, besides to deteriorate the detector performance, to artificially increase the data volume in a free-streaming data acquisition (DAQ) system. Our solution for minimization of such upshots has been the design of MSMGRPC prototypes with a direct flow of the gas mixture through the gaps between the resistive electrodes [2]. Flushing directly the active volume leads to a faster removal of the chemical pollutants that deposit around the spacers and on the surfaces of the resistive electrodes. Extensive aging tests of direct flow MSMGRPC prototypes demonstrated significant improvements brought by the new design. They were reflected in the reduced values of the dark currents and dark counting rates measured after irradiation, in comparison with a prototype with gas exchange via diffusion [3]. Further improvements were obtained by the replacement of the the continuous nylon line by discrete polyimide pad spacers in order to minimize the active area in contact with the spacers and consequently reduce further the noise rate localized around them.

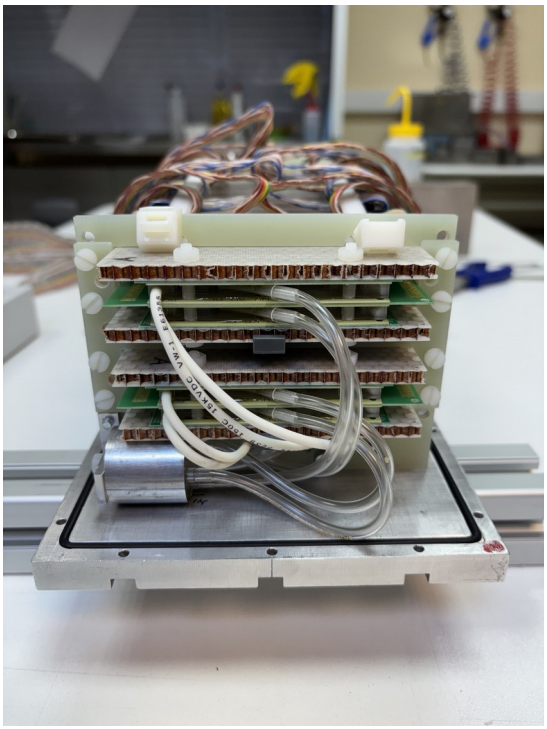

Fig.5 The two prototypes assembled on the back- panel of housing box

The first direct flow MSMGRPC prototype based on discrete spacers was assembled using 310 mm × 60 mm resistive electrodes and home made polyimide (kapton type) spacers of 200 μm thickness with a rectangular shape of 2 mm x 2 mm size. It will be called further P200. Searching on the market, we found commercially available polyimide spacers of 170 μm and a second prototype was assembled using them. It will be called further P170. The spacers were distributed with pitches of 30.7 mm along and of 28.5 mm across the length of the resistive electrodes. Both chambers have the highest granularity of the CBM – TOF wall, corresponding to 56 mm strip length (MRPC1a).

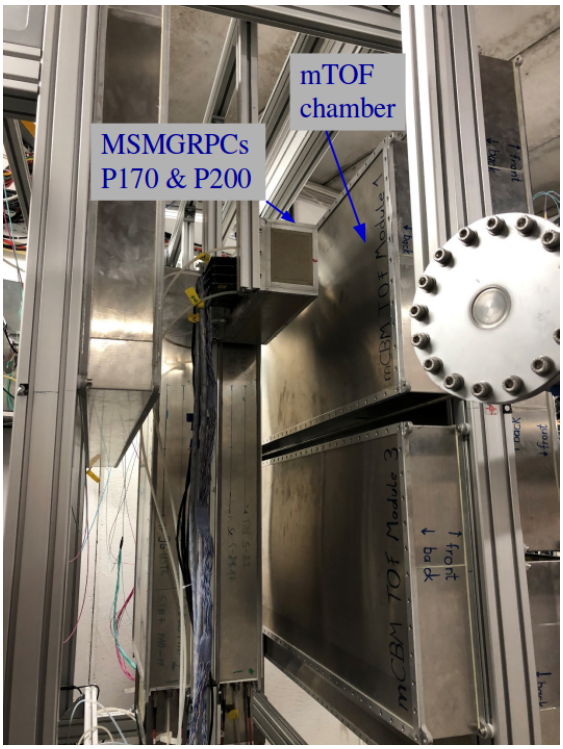

Fig.6 Photo of the box with the prototypes integrated in the experimental setup.

The results obtained in the aging investigations of these direct flow prototypes with discrete spacers exposed to a high X-ray flux, demonstrated very low values of the dark current and dark counting rate, even at lower gas flow rate [3] in comparison with the ones used for prototypes assembled using nylon line spacers.

A further step was to test the performance of the prototypes with a direct flow and polyimide discrete spacers in real operation conditions in the mCBM setup at SIS18/GSI.

The two MSMGRPC prototypes based on discrete spacers (P200 and P170) were installed in the mCBM experimental setup as shown in Fig. 6.

Each chamber was flushed directly through the gas gaps with a gas mixture of 97.5%$C_2H_2F_4$ + 2.5%SF_6. The strips were readout at the both ends by front-end electronics motherboards designed for the inner wall [4]. Each motherboard contains 4 PADI XI amplifier-discriminator ASICs and 8 self - triggered GET4 time-to-digital converters. The tests were performed using reaction products of a ^{197}Au beam of 1.2A GeV incident on a Au target. For the measurement of the efficiency and time resolution a four station tracking setup was defined (from upstream to downstream) by the beam reference detector (a strip diamond detector positioned in front of the target), a mTOF multi-gap resistive plate chamber with strip readout (270 mm x 300 mm active area) and the two P170 and P200 prototypes.

The efficiency of each of the two prototypes was obtained using as reference tracks reconstructed in the three out of the four stations of the tracking setup and looking for a reconstructed hit in certain time and space windows in the fourth station, considered detector under test (DUT). The efficiency as a function of the electric field in the gas gap (Fig. 7) shows a plateau around 95% for both prototypes. As expected, for the

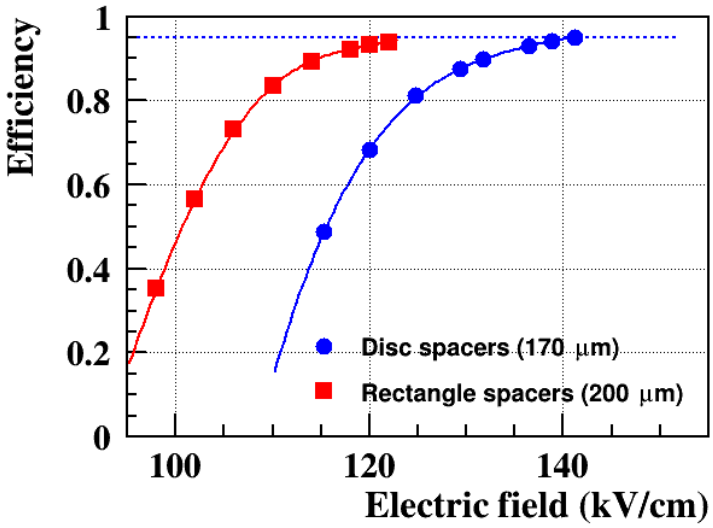

Fig.7 Efficiency as a function of the electric field in the gas gap. The error bars are contained within the size of the symbols.

thinner gap prototype P170, a higher field is needed in order to reach the same efficiency as with the P200 prototype. However, considering that the P200 prototype was the last one in the tracking setup, its efficiency measurement has been underestimated. Because it was not backed up by any other chamber, the reference tracks defined by the three stations in front of it could have tracks which already stopped in the P170 prototype. Therefore, the 95% efficiency measurement for P200 prototype is a conservative one. The measured time resolution was obtained as standard deviation of the Gauss function fitted to the distribution of the time difference between the measured and the expected time of arrival of particles in the chamber. The measured time was corrected for the rise time of the amplifying electronics (slweing corrections).

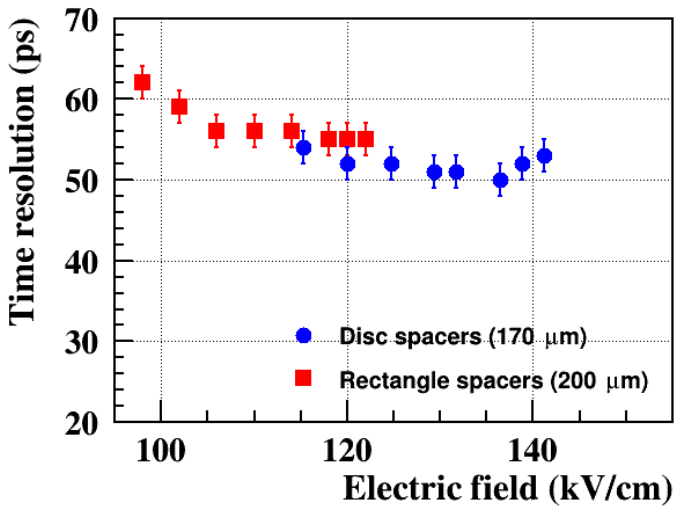

Figure 8: Time resolution as a function of the electric field in the gas gap

Fig. 8 shows the measured values of the time resolution as a function of the electric field in the gas gap, showing slightly better values for the chamber with thinner gas gaps, as expected. The slight deterioration of the time resolution in the region of the efficiency plateau for P170 chamber could be due to the smaller avalanches which grow enough in the stronger electric field, such that the small induced signals cross the threshold with a larger spread of the temporal response, not fully corrected by the slewing corrections.
Taking into consideration the results of the in-beam test presented above and the good behavior of the direct flow prototypes with discrete spacers in the previously performed aging investigations, this type of chambers will be implemented in the inner zone of the CBM-TOF wall. In the assembling of the MSMGRPCs for the inner wall will be used spacers of 200 μm thickness which better fits with the gain of the PADI XI ASIC, enlarging the efficiency plateau. The implementation of the chambers in the inner zone of the CBM - TOF will start with the assembling of the M0 module. This module is the most complex one, accomodating all three types of chambers of the CBM-TOF inner zone.

References:

1. D. Bartos et al., Ageing studies of Multi-Strip Multi-Gap Resistive Plate Counters based on low resistivity glass electrodes in high irradiation dose, Nucl. Instrum. Meth. A 1024 (2022) 166122. doi:10.1016/j.nima.2021.166122

2. M. Petris et al., High time resolution, two-dimensional position sensitive MSMGRPC for high energy experiments, Nucl. Instrum. Meth. A , 1045 (2023) 167621.

3. V. Aprodu et al., Aging suppression, high time resolution and 2d-position sensitive Multi-Strip Multi-Gap Resistive Plate Counter for high rate experiments, Nucl. Instrum. Meth. A , 1049 (2023) 168098. doi:10.1016/j.nima.2023.168098.

4. J. Frühauf et al., Hardware development for CBM ToF, CBM Progress Report 2012 (2013) 67.

2.2 CBM - TRD

A TRD2D demonstrator prototype was fully operated in the February-March 2025 data taking campaign at mCBM at the SIS18 facility of GSI. We took data continuously, together with the reference detectors STS for tracking and ToF for PID. The data processing for TRD2D is done fully within the collaboration software CbmRoot[2] for both online and offline processing. For the performance studies a dedicated package was developed in the CbmRoot framework[3] which can also provide QA plots for the reference detectors, for both measured and MC data.

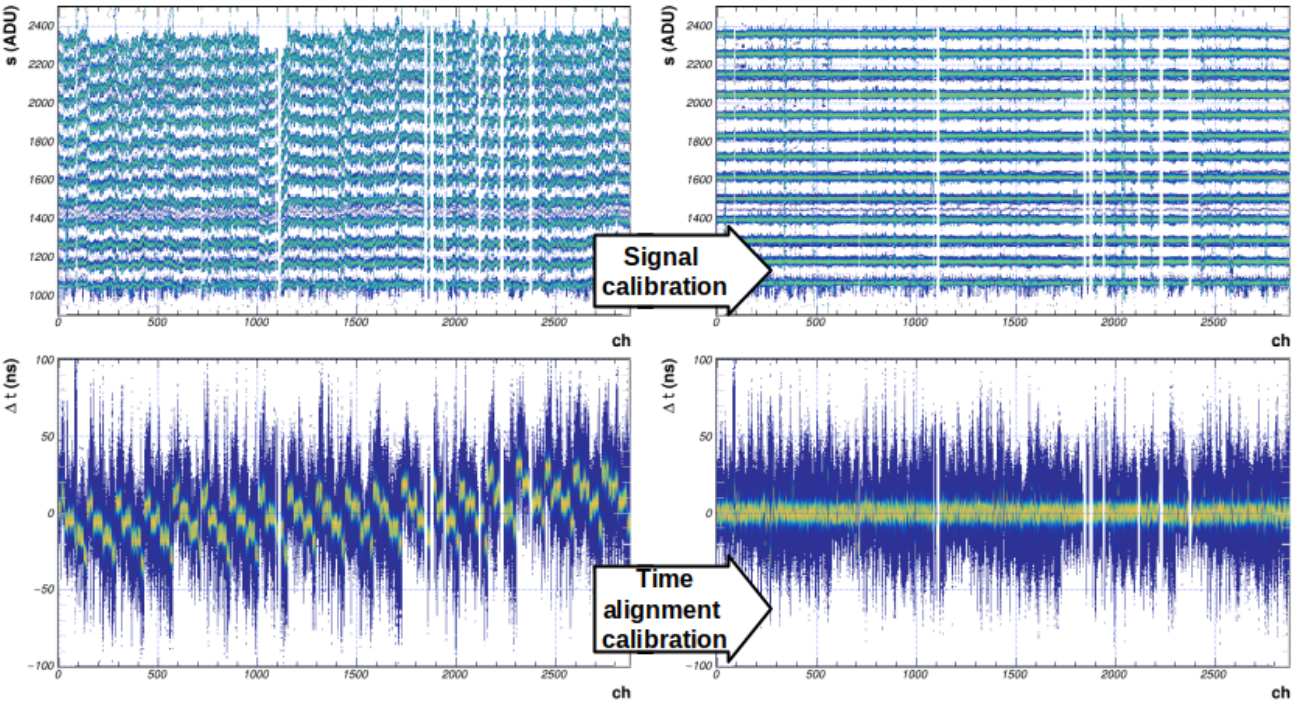

Figure 1: Calibration of the signal (top plots) and the time (bottom plots) responses of the TRD2D in the mCBM experiment.

The first step of realistic data processing exercised @mCBM was to apply the signal/time calibration at the level of online data unpacking. In Figure 1 we show the distribution of signals (top) and relative time (bottom) before (left) and after (right) the calibration. One can observe the result of calibration in removing the systematic fluctuation from FEE channel to channel while conserving the remaining fluctuations - due to construction process - which can be measured and propagated to the final observables uncertainties.

The second step of data preparation was to align STS sensors such that the reference tracks used in the TRD2D for hit attachment and position performance estimations are unbiased. The alignment procedure and its convergence will not be described here. In Figure 3 we show only one of the final results, the analysis of the residual distribution between tracks and hits, in the STS first two tracking stations - according to the marks in the figure. Each plot represent the correlation between the **position residuals in the horizontal (assigned as *x*) direction** between reconstructed hits in the STS sensor of reference and the track extra/interpolation from the other remaining two STS stations and the **hit attached to the track** in the sensor of reference. For each position in the sensor, marked on the horizontal axis, the profile of the distribution on the vertical axis is calculated and the mean (white) and sigma (yellow) is computed. Finally, the trend of mean/sigma values as function of its x position, in red/black straight lines, is used to quantify the alignment/error parametrization of the data. To estimate the intrinsic fluctuation of the data as opposed to the effects of imperfections in the measurements (missing and/or noisy channels, etc.)

2. https://git.cbm.gsi.de/computing/cbmroot
3. https://git.cbm.gsi.de/computing/cbmroot/-/blob/master/reco/qa/CbmRecoQaTask.cxx

we show, as one-to-one comparison, between measurements performed in run 3604[4] (left) and MC simulations with perfect alignment.

Some conclusions from Figure 3:

- Measurements are aligned with micrometer precision in all directions x, z and y (not shown).

- There are regions of the experimental setup which are damaged and their performance and efficiency are below expectations (MC) - clearly seen in sensor *e.g.* STS/U0 (top).

- values of the cumulative errors (hit+track) reported in black are reasonably well reproduced by MC (78.5/70.3, 40.2/32.4, 50.6/44.6 and 38.6/32.5), the difference being of "only" +15%.

After having the systematic effects of the reference tracks under relative control we can show, in Figure 3, the performance in position observables for the TRD2D in the same manner as described above for the STS detector in Figure 2.

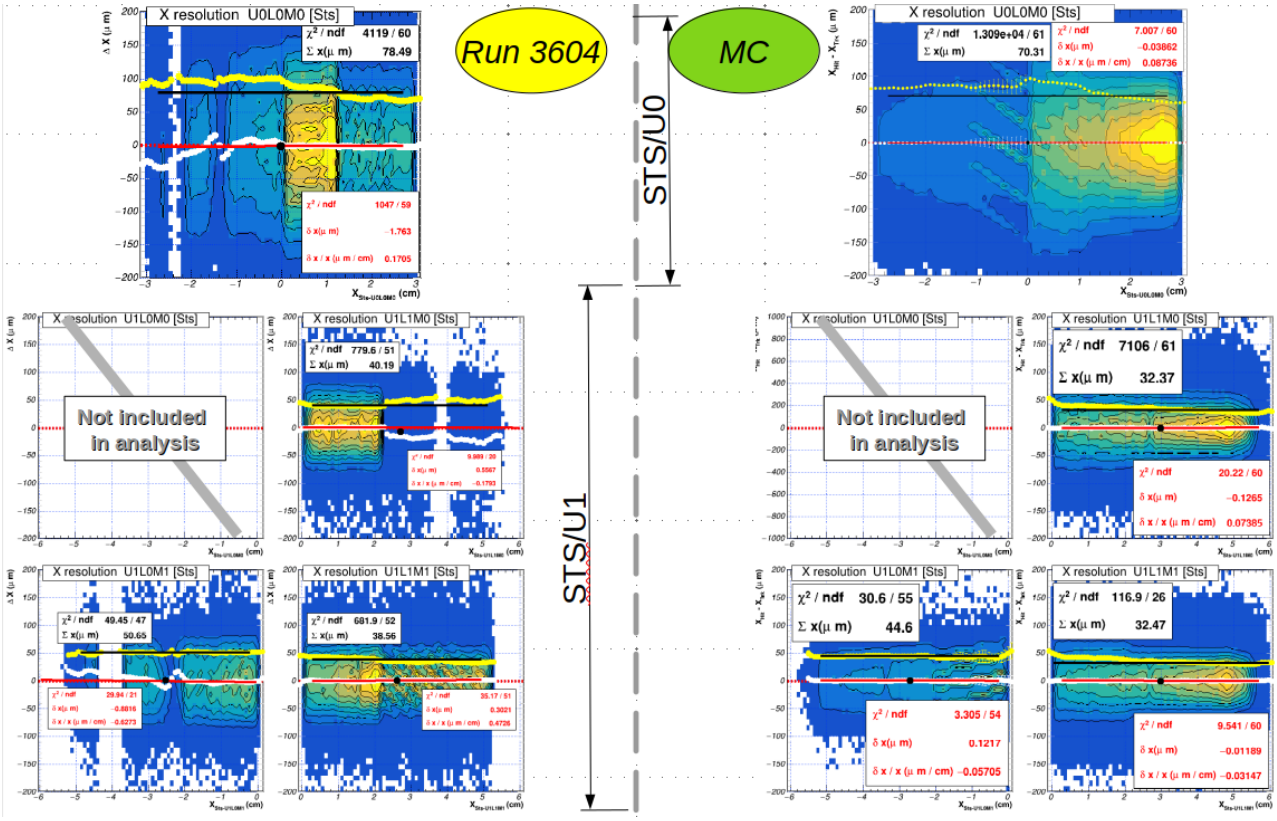

Figure 2: Track to Hit position residuals in the first two STS tracking units; A comparison between aligned measured (run 3604) data (left) and ideal MC simulations (right).

The efficiency and systematic effects observed on the measured data of TRD2D (Figure 3 left) is modulated by the STS system (see STS/U0 in Figure 2 top-left) with the best measured region for x_{TRD2D}(cm)=[0,8]. For this region we compare the position across pads (***x***) performance against ideal MC simulations (Figure 3 right).

4. Au-Au E_{kin}=1.23 AGeV @ ~ 10 MHz interaction rate

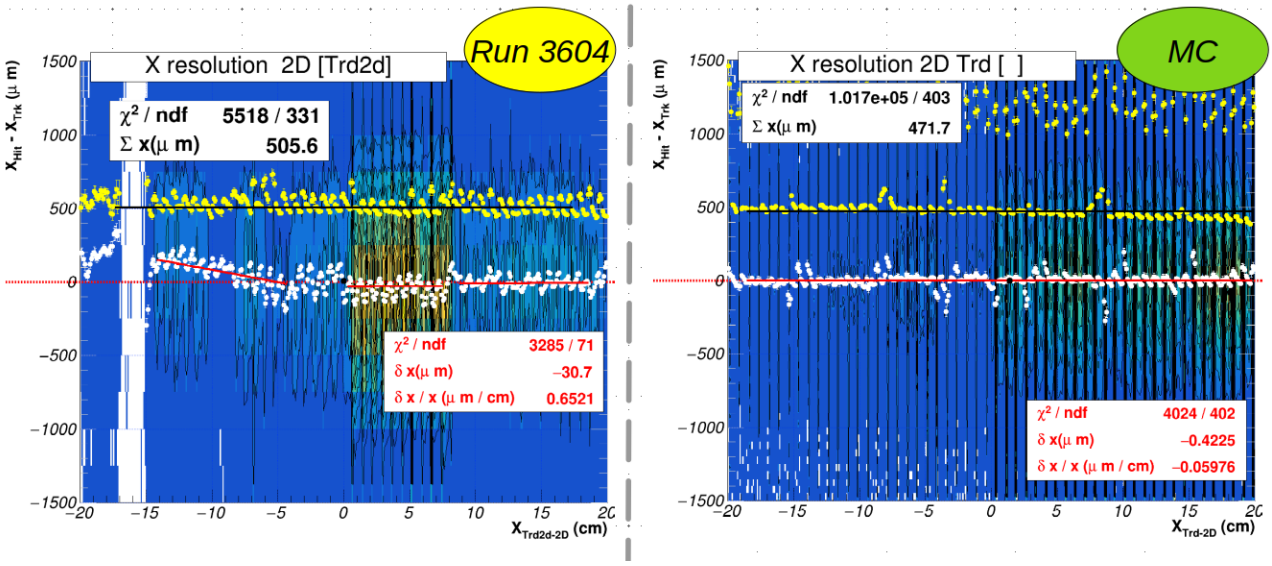

Figure 3: Track to Hit position residuals in TRD2D; Same comparison as in Figure 2.

Some conclusions from Figure 3:

- the residual mis-alignment of TRD2D for the x and z directions is on the level of few tens of microns induced partially by distinguishable mis-alignments in the STS.

- Track+Hit errors estimation show an overestimation in the measurements of only 7% *wrt.* the MC (505.6/471.7 μm) suggesting a good confidence in the estimated uncertainties used in the reconstruction algorithm.

- Systematic effects (white markers) in the measured data, seen as oscillations around the mean (red line) are larger than the corresponding effect seen in MC by few tens of microns suggesting further improvement scenarios for our current understanding of the detector in general and the demonstrator prototype in particular.

2.2.3 CBM - TRD-2D FEE

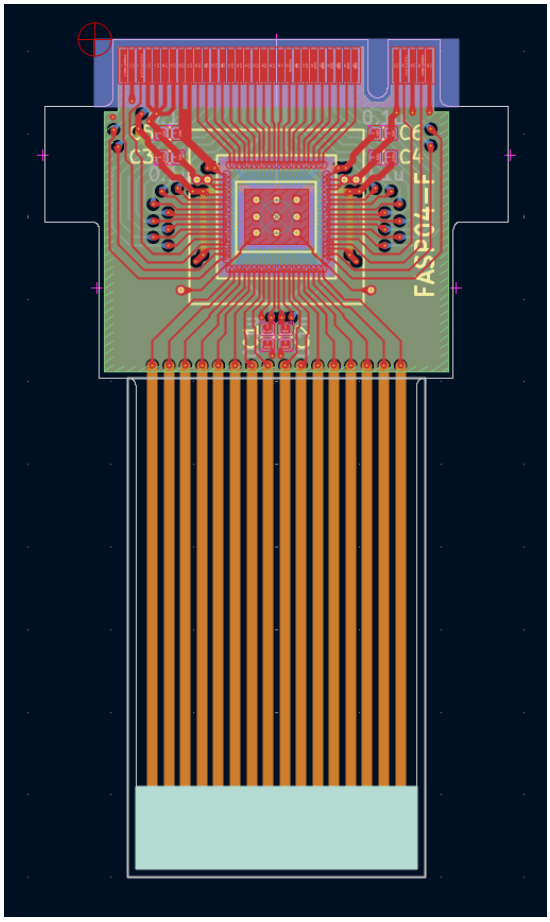

Using a field-replaceable FASP packaging, the development of a solution to test large amount of FASPs is simplified, as the FEE board used for the chambers (to be developed for the new FASP packaging) may also be used for the reading part of the chip testing. Only the part related to the signal injection need to be developed. Work on this is well under way, commercially available components and overall structure were identified, only the actual injection board have to be designed, in coordination with the design of the new FEE board.

As previously reported, in order to fix the observed issues with the “flip-chip” packaging of FASP, we decided to change the way the connection between the pad-plane and FEE is made. A new pad-plane using FFC/FPC connectors (instead of soldered FFC cables) was developed (previously reported).

The presence of FFC/FPC connectors on the pad-plane have several advantages, the most important one being the possibility to use for FASP a packaging “on the FFC cable”. A new substrate for FASP packaging was designed (image on the right). The FASP die is wire-bonded on the rigid part of a figid-flex PCB and covered with a glob-top. This method of bonding is widely used and provide the best yield. The flex part of the board consist in a “FPC cable” and is used to connect to the FFC/FPC connector on the pad-panel. The connection to the rest of FEE is provided by the upper board edge, using a card edge connector on the FEE board. The decoupling capacitors are also installed on this board, further reducing the required space on the FEE.

A major advantage of this packaging is that FASP is not soldered on the FEE, thus avoiding the observed reflow issues and also becoming “field-replaceable”. It would be possible to easily replace defective FASP without replacing the full FEE.

Also, as this packaging reduces the required space and the geometric constraints on the FEE board, it might be possible to use one (larger) FPGA instead of 3, as the current solution. This would reduce the cost and the dissipated power and it would simplify the firmware. This possibility is currently under investigation.

The firmware on both FEE and CRI boards was maintained, observed bugs were fixed. During the February-March 2025 mCBM campaigns the FEE operated almost without interventions.

The development of a new version of the firmware on the FEE started, aiming many optimizations and new features.

- Describe the progress in achieving the project goals
  - A final design of the CBM-TOF inner wall is available and ready to be implemented.
  - Direct flow MSMGRPCs based on discrete spacers and equipped with the FEE designed for the inner-wall, proved their performances; they will be implemented in the 12 modules of the CBM-TOF inner wall. The obtained results were published in a NIMA paper and presented at EuNPC2025 conference.
  - A software package for TRD-2D data analysis is integrated in the CBM software.
  - The firmware on both FEE and CRI boards was updated, observed bugs were fixed.
  - A simplified solution to test a large amount of FASPs was elaborated.

4. Deliverables

- Scientific reports

- *List of papers (preprints, journal, conference proceedings)*
  1. M. Petris, V. Aprodu, I. Deppner, V. Duta, J. Fruenhauf, N. Herrmann, M. Petrovici, A.Radu, E. Rubio, Radiation hard multistrip multigap resistive plate chamber architecture for low polar angles of the CBM - TOF wall, Nuclear Inst. and Methods in Physics Research A 1078(2025), 170580

- *List of talks of the group members (title, conference, date)*
  1. M. Petris et al., New timing Multi-Strip Multi-Gap Resistive Plate Chamber architecture with aging suppression for high interaction rate experiments, European Nuclear Physics Conference, Caen, France, 22 – 26 September 2025

  List of presentations at the CBM Collaboration Meetings:

  1. M. Petris et al., Status and plans of the CBM-TOF inner wall activities
     45th CBM Collaboration Meeting, GSI Darmstadt, 16 – 21 February, 2025
  2. A. Bercuci et al., TRD2D status
     45th CBM Collaboration Meeting, GSI Darmstadt, 16 – 21 February, 2025
  3. A. Bercuci et al., TRD Inner modules
     45th CBM Collaboration Meeting, GSI Darmstadt, 16 – 21 February, 2025
  4. M. Petris et al. CBM-TOF inner wall status overview
     46th CBM Collaboration Meeting, Lanzhou, China, Oct 19 – 24, 2025
  5. A. Bercuci et al., TRD-2D status and plans
     46th CBM Collaboration Meeting, Lanzhou, China, Oct 19 – 24, 2025

- Other deliverables (TDR, patents, books etc.).

5. Further group activities (max 1 page)

- Collaborations, local synergies, education, outreach
  5.1 CBM-TOF
  - One master student is integrated in the local TOF group, Master Thesis is in progress.
  - Two bachelor students joined the TOF group after partcipation in the Summer Student Program, finalized with two Reports for the Physics Faculty of Bucharest University.
  - participation with 4 MSMGRPCs in the cosmic ray setup of Heidelberg CBM-TOF group

5.2 CBM-TRD-2D

- increased the synergies with the CBM-TRD groups by adopting similar design solutions for the entrance window and gas inlets rendering a uniform gas infrastructure and description of the transition radiation yield.

- joined the efforts of the Muenster TRD group to design and construct a new device for the QA of the anode/cathode wire position/tension determination.

- developed internal collaborations with other groups inside IFIN-HH for manufacturing components and tools needed for the construction of the TRD2D detectors.

- 1 Politechnica University student participated to the Summer Student program in the TRD2D group

- 1 Master student from Faculty of Physics, University of Bucharest is joining TRD2D group.

Outreach:

Visit of pupils and teachers of "Clisura Dunarii" High School, on 8th of May 2025 in HPD (https://www.facebook.com/IfaInstitut/posts/vizita-elevilor-%C8%99i-profesorilor-de-la-liceul-tehnologic-clisura-dun%C4%83rii-din-data/1281836670616846/).

Visit of the independent experts of the board for the evaluation of the performance of scientific research and technological development activity of IFIN-HH, on 12th of November 2025.

Visit of members of members of the CBM Management Team in HPD, (7 – 12 of December, 2025).

7. Research plan and goals for the next year (max 1 page)

All components (mechanical supports, cover, backpanel, signal cables) of the first module of the CBM-TOF inner zone, M0 module, will be manufactured. The assembling and testing of the chambers of this module will start (all components are already manufactured) and they will be implemented in the M0 module. The assembled M0 module will be tested at SIS18/GSI Darmstadt.

A number of design updates and construction tools are being developed such that a stable and reliable assembling procedure for TRD-2D chambers will be set in place. A list of standardized QA tests are being defined, both locally and at the level of CBM-TRD to ensure a uniformly quantifiable and operational TRD for CBM. The performances of the TRD-2D wrt. the position and energy resolution will be studied further by using the PID information derived from $\Lambda \rightarrow p + \pi$ reconstruction together with BMon, STS and ToF., using existing experimental data. Participation to a high rate test and data taking together with the STS and TRD-STD at SIS18 is foreseen.

Multi-differential studies with theoretical models of physics observables sensitive to new phases of QCD matter at high baryonic densities will be performed.